Raman linewidths of optical phonons in 3*C*-SiC under pressure: First-principles calculations and experimental results

A. Debernardi, C. Ulrich, K. Syassen, and M. Cardona
Max-Planck-Institut für Festkörperforschung, Heisenbergstrasse 1, D-70569 Stuttgart, Germany
(Received 6 August 1998)

We have studied the pressure dependence of the linewidths of the longitudinal and transverse optical phonons at the Brillouin-zone center in 3*C*-SiC. Raman measurements at 6 K, which cover the pressure range up to 15 GPa, are in good agreement with first-principles calculations also reported here. These results differ considerably from previous experimental data. While the linewidth of the transverse mode remains practically unchanged within our pressure range (up to 35 GPa for the calculation), that of the longitudinal mode shows a monotonic increase up to 26 GPa, decreasing abruptly above this pressure. The mechanisms responsible for this anomalous behavior are identified and discussed. Experimental and theoretical results concerning the pressure dependence of phonon frequencies and related quantities complete the work.
[S0163-1829(99)02409-1]

I. INTRODUCTION

Silicon carbide is the only IV-IV semiconductor which forms long-range ordered polytypes (meta)stable at room temperature.[1] Since SiC is one of the most promising materials for electronic and optical device applications,[2] especially at high temperatures, there has been a large interest in the investigation of its physical properties. This includes detailed experimental[3–11] and theoretical[12–17] studies of the lattice dynamics and changes induced under applied hydrostatic pressure.

Among the lattice-dynamical properties of interest we find the decay time of phonons, which controls the formation and evolution of a hot (nonequilibrium) phonon population when phonons are emitted by high-density excited carriers decaying towards their ground state.[18] The decay time of a given phonon can be experimentally obtained from the full width at half maximum (FWHM) of the corresponding Raman line. Olego and Cardona investigated the temperature dependence of the Raman linewidths of the zone-center optical modes in 3*C*-SiC,[5] which has the zinc-blende structure. A first-principles study of the dependence of the Raman linewidths on temperature and isotopic composition and a comparison to available experimental data is presented in Ref. 19. Olego and Cardona also investigated the pressure dependence of Raman linewidths at room temperature using a gasketed diamond anvil cell. They found that the linewidths of long-wavelength optical phonons, both transverse and longitudinal, increase sharply for pressure above 10.6 GPa.[3] This effect was not observed in later Raman studies of epitaxial layers of 3*C*-SiC by Kobayashi *et al.*[10]

In this work we report the pressure dependence of the linewidths of transverse optical (TO) and longitudinal optical (LO) phonons obtained by *ab initio* electronic structure techniques and, experimentally, by *low-temperature* Raman spectroscopy. We report the calculated FWHM of transverse and longitudinal optical Raman-active phonons of 3*C*-SiC under pressures up to about 35 GPa at zero temperature and the pressure dependence of the FWHM of Raman lines at 6 K for both longitudinal and transverse optical phonons measured up to 15 GPa. In accordance with our calculated results, the anomalous line broadening reported in Ref. 5 is not confirmed by the present experiment, where pressure conditions were essentially hydrostatic due to the use of helium as a pressure medium.

This paper is organized as follows: first we give a short account of the general theory of phonon lifetimes, describe the computational methods used in this work, and give some experimental details (Sec. II). We then present experimental and theoretical results for the pressure dependence of phonon frequencies and briefly discuss the LO-TO splitting and related properties (Sec. III). Then we turn to the results for the pressure dependence of the phonon lifetimes and a detailed analysis of the anharmonic decay channels of optical phonons based on the theoretical results (Sec. IV).

II. THEORY AND EXPERIMENT

A. General theory of phonon lifetime

The natural width of a Raman phonon line of a perfect crystal is given by its probability to decay into phonons of lower energy, i.e., by the inverse lifetime of a phonon. In our case we consider the decay of an optical phonon at the zone center at zero temperature, so only decay into two phonons of opposite wave vector $\mathbf{q}$ is allowed by the conservation of the momentum. At zero temperature the FWHM of the LO mode at the zone center reads

$$2\Gamma = \frac{\pi}{\hbar^2}\sum_{\mathbf{q},j_1,j_2}\left|V_3\begin{pmatrix}\mathbf{0}, & \mathbf{q}, & -\mathbf{q}\\ \mathrm{LO}, & j_1, & j_2\end{pmatrix}\right|^2 \times \delta(\omega_{\mathrm{LO}}(\mathbf{0})-\omega_{j_1}(\mathbf{q})-\omega_{j_2}(-\mathbf{q})), \quad (1)$$

where the indices j_1, j_2 run over the various phonon branches. The anharmonic matrix elements V_3, appearing in Eq. (1), are essentially third derivatives of the total energy per unit cell with respect to the phonon displacements[20] which are computed using density-functional perturbation theory according to the scheme proposed in Refs. 21 and 22.

The Dirac delta function takes into account conservation of energy. The scheme represented by Eq. (1), which was used in Ref. 23 to compute the phonon linewidths of elemental semiconductors with the diamond structure, can be applied without modification to compute the linewidths of transverse optical modes in zinc-blende-type materials.

To calculate the matrix elements V_3 for the LO phonon, one has to take into account that the displacements from the equilibrium positions corresponding to a longitudinal phonon at the zone center create a long-range macroscopic electric field which couples with the phonons (for the TO phonons only short-range effects need to be considered). The difference in the electron density response to a longitudinal and a transverse optical phonon displacement in the long-wavelength limit for zinc-blende-type materials has been discussed by Resta.[24] He showed that, to first order in the phonon displacement, the electron density induced by a LO phonon at the zone center differs from the TO phonon by an amount Δn_E which is proportional to the density response given by the macroscopic component of the electric field created by the phonon displacement. The contribution of Δn_E to the LO frequency is, in general, small compared to the frequency itself (e.g., in 3*C*-SiC it is $\sim 8\%$ of ω_{LO}), however, it is important in the computation of phonon-dispersion relations since it determines the LO-TO splitting. The microscopic theory of LO-TO splitting was derived in the pioneering article of Pick, Cohen, and Martin.[25] To the best of our knowledge no attempt has been made to treat in the same way anharmonic contributions.

Since the phonon linewidth is mainly governed by *kinematic* processes[23,26] (i.e., by conservation of energy and wave vector) the simplest approximation corresponds to including the Δn_E for the computation of the phonon frequencies and neglecting it in the calculation of the anharmonic contribution V_3. This zero-field anharmonic approximation (ZFAA) was recently used to study the zone-center LO phonons in III-V semiconductors,[26] giving results in very good agreement with experimental data.

B. Computational scheme

We performed calculations in the density-functional framework using the local-density approximation and the pseudopotential technique.[27,28] The phonon frequencies are computed by density-functional perturbation theory according to the scheme of Ref. 29. The electron density was expanded in a plane-wave basis set with a kinetic energy cutoff of 44 Ry. This cutoff ensures an accurate convergence of the computed quantities over the whole pressure range. We have used the norm-conserving pseudopotentials of Ref. 23, to which the reader is referred for further details, and the local-density approximation for the exchange and correlation energy, as calculated by Monte Carlo techniques by Ceperley and Alder,[30] with the interpolation proposed by Perdew and Zunger.[31] The Brillouin-zone (BZ) integration over electronic states necessary to compute the dynamical matrix was performed using the special point technique[32] with a (8,8,8) Monkhorst-Pack[33] integration mesh which corresponds to the 10-points Chadi-Cohen set[32] in the irreducible wedge. The reciprocal space summation (integration) over phonon states which appears in Eq. (1) was performed with the tetrahedron method,[34,35] using approximately ~ 1500 points in the irreducible wedge of the BZ. The integrand is calculated on a much coarser uniform mesh and then Fourier interpolated on the finer grid in the same way as in Ref. 26. We minimize the total energy per unit cell calculated at different volumes, then the data are fitted with the Murnaghan equation of state[36] to obtain (experimental data are given in parentheses): the equilibrium lattice constant $a_0 = 4.338$ Å, (4.358 Å),[37] the bulk modulus $B_0 = 220$ GPa, $(227 \pm 3$ GPa),[7] and its derivative $B_0' = 3.62$, (4.1 ± 0.1).[7] All the theoretical results presented in this work are computed at $T = 0$.

C. Experimental procedures

3*C*-SiC small bulk single crystals ($\sim 0.5 \times 0.5 \times 0.5$ mm) were grown at Westinghouse research laboratories by Choyke. In order to fit into the gasket of a diamond-anvil high-pressure cell, the samples were mechanically polished to a thickness of about 25 μm and then cut into pieces of about 80×80 μm^2 in size. Raman-scattering experiments were performed in backscattering geometry at a temperature of 6 K. In order to ensure the best possible hydrostatic conditions, helium was used as the pressure transmitting medium and the pressure was always changed at room temperature, where He is fluid up to 11.3 GPa.[38] The pressure was measured *in situ* to within ± 0.03 GPa experimental error using the ruby luminescence method[39] with temperature correction of the pressure calibration according to Ref. 40. The 647.1 nm line of a Kr^+ laser was used for excitation. In order to avoid sample heating, the power density was kept below 400 W/cm^2. In recent studies of the optical phonon lifetime in Ge,[41] it was observed that the Raman linewidth showed a dependence on laser energy, an effect which is related to the small optical penetration depth of visible light in Ge. We note that for all experiments performed on 3*C*-SiC under pressure there was no change of phonon linewidth for different laser energies below the optical band gap ($E_G = 2.416$ eV, for the pressure dependence, see Ref. 42).

The scattered Raman light was dispersed by a Jobin Yvon T64000 spectrometer operated in the subtractive-dispersion mode of the filter stage and measured using multichannel detection. The experimental Raman line shape $I(\omega)$ (ω is the Raman shift) corresponds to a convolution of the true Raman profile $L(\omega)$ and the spectrometer profile $G_n(\omega)$:

$$I(\omega) = \int_{-\infty}^{\infty} G_n(\omega') \cdot L(\omega - \omega') d\omega'. \qquad (2)$$

The index n indicates that the area under $G_n(\omega)$ is normalized to one. The spectrometer profile and calibration were determined by measuring, for each Raman spectrum, an additional spectrum of a nearby emission line of a Ne calibration source. The entrance and the intermediate slits were kept at 100 μm. Under these conditions, $G_n(\omega)$ was found to be well approximated by a Gaussian with a FWHM of 0.83(3) cm^{-1}. In the absence of inhomogeneous broadening[19] and for weak coupling of the phonon mode to other elementary excitations, the true Raman profile $L(\omega)$ is expected to be of the Lorentzian form of width 2Γ. Thus, $I(\omega)$ corresponds to the convolution of a Lorentzian and a

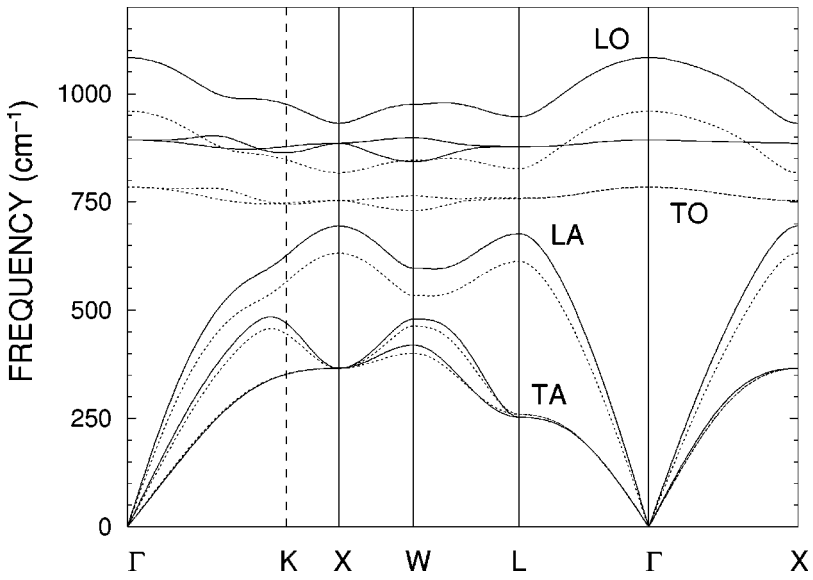

FIG. 1. Theoretical phonon dispersions of 3C-SiC along the main symmetry directions at ambient pressure (dotted lines) and at $P=33.5$ GPa (continuous lines).

Gaussian, which is known as the Voigt line shape.[43] Thus, to determine the Lorentzian linewidths, the measured spectra were fitted with the Voigt profile using a fixed Gaussian width for the independently determined spectrometer broadening. For an illustration of the linewidth determination we refer to Fig. 3 of Ref. 41. In the present work, the spectrometer broadening is significantly smaller than the observed Raman linewidths. Thus, the 2Γ values do not depend very much on the deconvolution procedure. The frequency and linewidth data presented below and their error bars correspond to the average and the standard deviation, respectively, of at least six spectra for each pressure point.

III. PHONON FREQUENCIES

A. Pressure dependence

In this section we present the experimental and theoretical results concerning the pressure dependence of the phonon frequencies at the BZ center[44] and compare them with each other in order to assess the reliability of the theoretical model.

In order to facilitate subsequent discussions, we display in Fig. 1 the computed phonon branches along the main symmetry directions at ambient pressure (dotted line) which reproduce the results of Ref. 13 obtained with the same technique. In the same figure we also report the phonon dispersion computed at $P=33.5$ GPa (continuous line) which corresponds to the upper limit of the pressure range of our theoretical study.

Figure 2 shows first-order Raman spectra of 3C-SiC at different pressures up to 15 GPa measured at $T=6$ K. With increasing pressure both Raman lines, LO and TO, shift to higher frequencies. No extra lines are observed which would indicate the presence of other polytypes of SiC. A very weak asymmetry is observed for both Raman lines; their origin has not been identified. These asymmetries remain unchanged under pressure. The intensities of the peaks decrease by a factor of 2 in the pressure range up to 15 GPa, while the intensity ratio between the LO and TO peaks remains constant.

The results for the pressure dependences of the frequencies of the LO and TO modes are displayed in Fig. 3. The filled (open) symbols refer to measurements for increasing (decreasing) pressure. The pressure shifts are fully reversible. The linear and quadratic pressure coefficients obtained by fitting a quadratic relation to the experimental data are reported in Table I,[45,41,7,46] which also lists the mode Grüneisen parameters

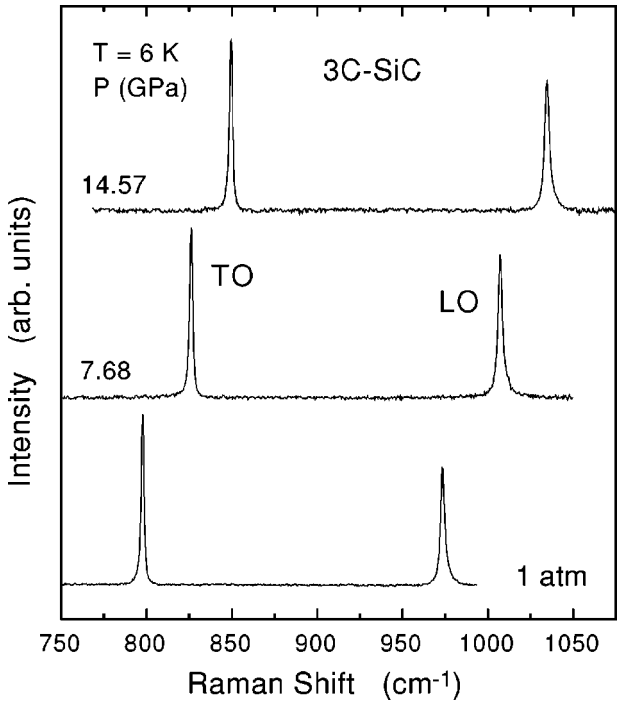

FIG. 2. Normalized low-temperature ($T=6$ K) Raman spectra of 3C-SiC at different pressures.

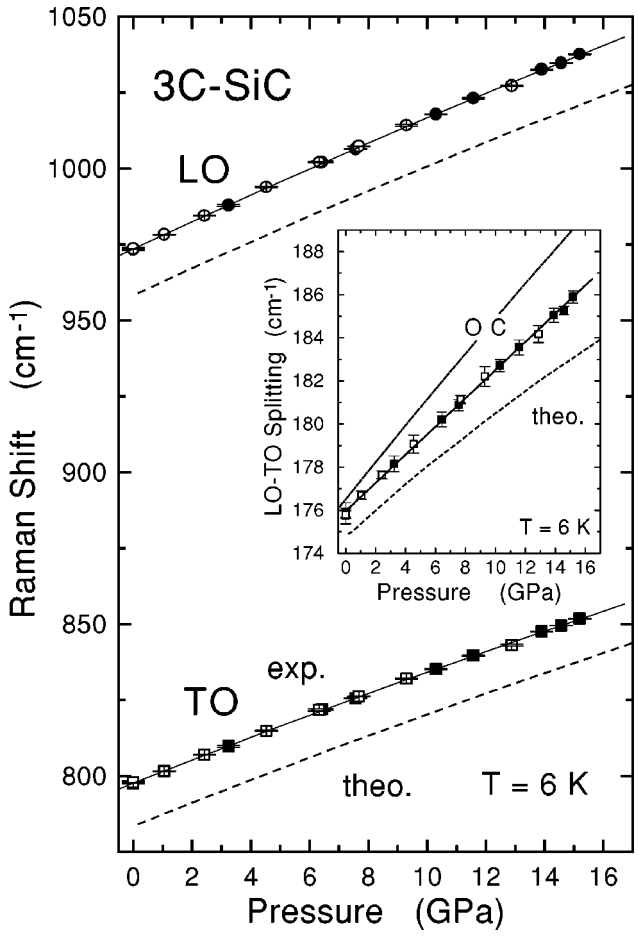

FIG. 3. Zone-center LO and TO phonon frequencies of 3*C*-SiC vs pressure. The symbols represent experimental data, the solid lines correspond to results of fits to the data, and the dashed lines represent the first-principles theoretical results. Closed and open symbols are used for increasing and decreasing pressure, respectively. The inset shows the difference between LO and TO frequencies as a function of pressure using the same symbols. The line marked ''OC'' in the inset refers to the experimental data of Ref. 4.

$$\gamma_G = -\frac{\partial \ln \omega}{\partial \ln V} \tag{3}$$

evaluated at zero pressure, i.e.,

$$\gamma_G = \frac{B_0}{\omega_0}\frac{\partial \omega}{\partial P}. \tag{4}$$

Previously measured values of Grüneisen parameters[6,4,7] differ by less than 3% from the present results. Olego and Cardona[4] have used an average bulk modulus of $B_0 = 321.9$ GPa for Si and C and obtained $\gamma_{LO} = 1.56(1)$ and $\gamma_{TO} = 1.56(1)$. Correction of their results using the bulk modulus of Ref. 7 gives $\gamma = 1.10$ for both the TO and LO modes.

Raman experiments of Liu and Vohra[11] on 6*H*-SiC at pressures up to 95 GPa revealed a decrease of γ_G with increasing pressure. From our high-resolution hydrostatic measurements for 3*C*-SiC up to 15 GPa, there is no indication of a sublinear pressure dependence of γ_G. The change in the mode Grüneisen parameter in Ref. 11 possibly results from nonhydrostatic experimental conditions. Our first-principles calculations predict, however, a linear decrease of the mode Grüneisen parameters with increasing pressure, in agreement with the previous experimental results.[7,11]

TABLE I. Pressure dependence of zone-center optical phonon frequencies of 3*C*-SiC. The results refer to fits of quadratic functions to experimental data. Phonon frequencies ω are in cm^{-1}, pressure P in GPa (all parameters are evaluated at zero pressure). For comparison, related data are listed for the zone-center modes of diamond, Si, and Ge. The last two columns give the mode Grüneisen parameters γ_G and the bulk moduli B_0 (in GPa) used to calculate γ_G.

	ω_0	$d\omega/dP$	$1/2(d^2\omega/dP^2)\times 10^2$	γ_G	B_0 [c]
TO(Γ)	797.7(1)	3.88(4)	−2.2(3)	1.105(5)	227
LO(Γ)	973.6(2)	4.59(5)	−2.6(4)	1.072(5)	227
LO-TO	175.9(3)	0.654(7)			
C(dia) [a]		2.90(5)		0.96(3)	442
Si [b]	523.9(1)	5.10(4)	−6.2(4)	0.96(1)	99.0
Ge [b]	304.6(1)	4.02(7)	−5.9(8)	1.00(1)	75.8

[a]Reference 45.
[b]Reference 41.
[c]References 7 and 46.

The calculated pressure coefficients and mode Grüneisen parameters for the zone-center optical modes as well as some of the zone-boundary modes are listed in Table II. The results of the *ab initio* calculations for the absolute TO(Γ) and LO(Γ) mode frequencies agree to within 1.5% percent with the experimental data, and the pressure shifts also are in excellent agreement with experiment. This is also demonstrated by the dashed lines in Fig. 3, which represent the theoretical results for the pressure shift of the LO and TO mode and for the LO-TO splitting.

While in a Raman experiment only zone-center modes are accessible, the first-principles technique permits calculation of phonon frequencies throughout the entire Brillouin zone. The degree of accuracy of our calculation in reproducing the phonon branches is expected to be the same as found for the frequencies at zone center. From Fig. 1 we notice a large increase of the longitudinal acoustic (LA) phonon frequency

TABLE II. Phonon frequencies for 3*C*-SiC and their pressure coefficients and Grüneisen parameters obtained from first-principles calculations (all parameters are evaluated at zero pressure). Phonon frequencies ω are in cm^{-1}, pressure P in GPa.

Mode	ω_0	$\partial\omega/\partial P$	$1/2(\partial^2\omega/\partial P^2)\times 10^2$	γ_G
TO(Γ)	783.7	3.813	−1.631	1.084
LO(Γ)	958.5	4.417	−2.033	1.019
TA(X)	366.0	0.155	−0.446	0.121
LA(X)	630.9	2.253	−1.106	0.806
TO(X)	752.2	4.653	−1.941	1.384
LO(X)	817.6	3.990	−1.615	1.090
TA(W)	400.8	0.814	−0.747	0.482
TA(W)	464.0	0.693	−0.691	0.357
LA(W)	533.9	2.259	−1.092	0.954

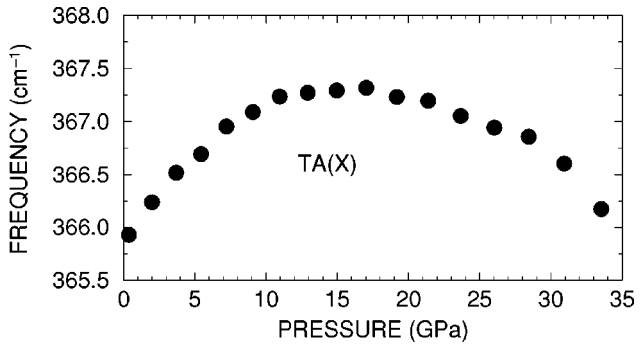

FIG. 4. Theoretical pressure dependence of the frequency of the TA phonon mode of 3*C*-SiC at the X point.

at the L point and a softening of the transverse acoustic (TA) phonons at the same point, in agreement with the experimental results of Ref. 8.

Especially interesting are the calculated results for the pressure dependence of the TA mode frequency at the X point, which are displayed in Fig. 4. The frequency changes very little with pressure: it first increases by 1.5 cm^{-1} for pressures up to $\sim$17 GPa and then decreases above this pressure. This behavior may be related to the fact that the Grüneisen parameter of this mode is positive for diamond whereas it is negative for silicon.[47] SiC must therefore be a borderline case, where the pressure coefficient of the TA mode is small and changes sign with increasing pressure. In Table II we also have presented the pressure dependence of the acoustic modes at W, important for the determination of the exact pressure at which an anomaly appears in the FWHM of the LO mode (see below).

B. LO-TO splitting

In contrast to the behavior displayed by the majority of the other zinc-blende semiconductors,[47] the LO-TO splitting increases with increasing pressure. This is shown in the inset of Fig. 3, where experimental and theoretical results are displayed.

The LO-TO splitting results from the macroscopic electric field associated with the LO phonon displacement. In a zinc-blende crystal it is related to Born's transverse effective charge Z^* through the relation

$$\omega_{\mathrm{LO}}^2-\omega_{\mathrm{TO}}^2=\frac{4\pi N_d Z^{*2}}{\epsilon_\infty \mu \Omega}, \tag{5}$$

where ϵ_∞ is the optical dielectric constant, μ is the reduced ionic mass, and N_d/Ω is the density of the anion-cation dipole pairs per unit-cell volume. The increase of the LO-TO splitting and therefore the increase of Born's transverse effective charge can be related to an increase of the ionicity of SiC under pressure,[4,48] which is in contrast to the behavior of other zinc-blende-type semiconductors. It can be explained by a charge transfer from Si to C due to the strong $2p$ potential of the C atom which results from the lack of p electrons in the carbon core.[12,48]

In our first-principles calculation we have computed Z^* and ϵ_∞ using density-functional perturbation theory[29] and the LO-TO splitting using Eq. (5). The theoretical results are presented in Table III together with the first and second derivatives with respect to pressure. At ambient pressure we reproduce the theoretical results obtained in Ref. 13. The pressure derivatives of Z^* and ϵ_∞ reported here are similar to those obtained in Refs. 15 and 17. The small differences are probably due to the fact that we have used a larger kinetic energy cutoff to take into account that the dielectric constant usually converges much more slowly than the force constants.

The Born effective charge calculated from the experimental LO-TO splitting using $\epsilon_\infty=6.52$ (quoted in Ref. 4) is $Z^*=2.681(0)$, which must be compared to our *ab initio* result of $Z^*=2.7220$. In order to determine the pressure dependence of Z^* from the experimental LO-TO splitting, one needs to know the pressure dependence of ϵ_∞. To the best of our knowledge this quantity has not been measured. Using the theoretical value of $\partial\epsilon_\infty/\partial P=-1.04\times10^{-2}$ GPa^{-1}, we obtain the ''experimental'' value of $\partial Z^*/\partial P$ and the corresponding volume coefficient γ_{Z^*} ($\gamma_{Z^*}=-\partial \ln Z^*/\partial \ln V$) as listed in Table III.

All theoretical calculations predict a sublinear pressure dependence of the LO-TO splitting with a tendency towards

TABLE III. Electronic dielectric constant, Born's transverse effective charge and their pressure coefficients for 3*C*-SiC obtained from theoretical and experimental results (all parameters are evaluated at zero pressure). Pressure P is in GPa.

	ϵ_∞	$\partial\epsilon_\infty/\partial P\times10^2$	$1/2(\partial^2\epsilon_\infty/\partial P^2)\times10^4$	$-\partial \ln \epsilon_\infty/\partial \ln V$	Ref.
Expt.	6.52				37
Theor.	6.96	-1.04	0.942	-0.354	This work
Theor.	7.02	-1.30	1.463	-0.342	15
Theor.	7.005			-0.3	16
	Z^*	$\partial Z^*/\partial P\times10^2$	$1/2(\partial^2 Z^*/\partial P^2)\times10^4$	$-\partial \ln Z^*/\partial \ln V$	Ref.
Expt.	2.681	0.331[a]		0.280[a]	This work
Theor.	2.722	0.296	-0.194	0.250	This work
Theor.	2.72	0.324	-0.270	0.270	15
Theor.	2.73	0.302	-0.216	0.251	14
Theor.	2.701	0.324	-0.270	0.272	16

[a]From expt. LO-TO splitting and calc. $\partial\epsilon_\infty/\partial P$.

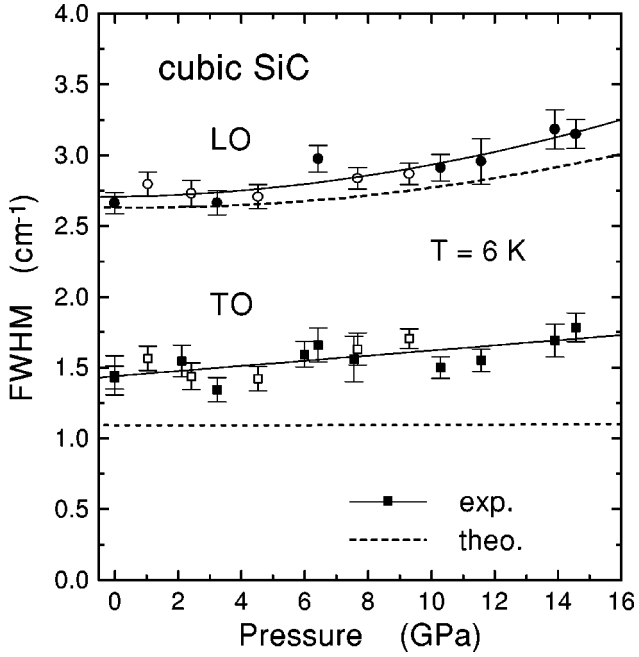

FIG. 5. Experimental (symbols) and theoretical (dashed line) results for the widths of zone-center optical modes of 3*C*-SiC under pressure. Closed and open symbols refer to increasing and decreasing pressure, respectively.

saturation at pressures above 50 GPa. In the pressure range covered by the present experiment and within experimental error, we find no deviation from a linear pressure dependence (see inset in Fig. 3). High-pressure Raman spectra of 6*H*-SiC were interpreted in terms of a decrease of the LO-TO splitting at pressures above 50 GPa.[11] It is not clear at this point, if this effect indicates a decrease of the Born effective charge or resulted from nonisotropic stress components.

IV. PHONON LINEWIDTHS AND DECAY CHANNELS

A. Pressure dependence of linewidths

Figure 5 shows the experimental results for the pressure dependence of the LO and TO phonon linewidths for pressures up to 15 GPa. The filled and open symbols refer to measurements for increasing and decreasing pressure, respectively. The pressure dependence is fully reversible. This shows that the application of pressure did not result in a formation of defects.

The measured zero-pressure linewidths [$2\Gamma_{TO}=1.44(5)$ cm^{-1} and $2\Gamma_{LO}=2.69(6)$ cm^{-1}] are significantly smaller than the previously measured low-temperature values[5] $2\Gamma_{TO}=2.0(2)$ cm^{-1} and $2\Gamma_{LO}=3.8(2)$ cm^{-1}. Our results under pressure also differ from the experimental data (taken at room temperature) presented in Ref. 3. In this reference the FWHM is shown to increase rather sharply at about 10.6 GPa, for both longitudinal and transverse optical phonons. This effect must have been due to the freezing of the methanol-ethanol mixture used as transmitting medium which is known to introduce anisotropic and inhomogeneous stains, resulting in a large increase of the experimental FWHM of both LO and TO phonon lines. We note that more recent Raman measurements[10] on epitaxially grown 3*C*-SiC

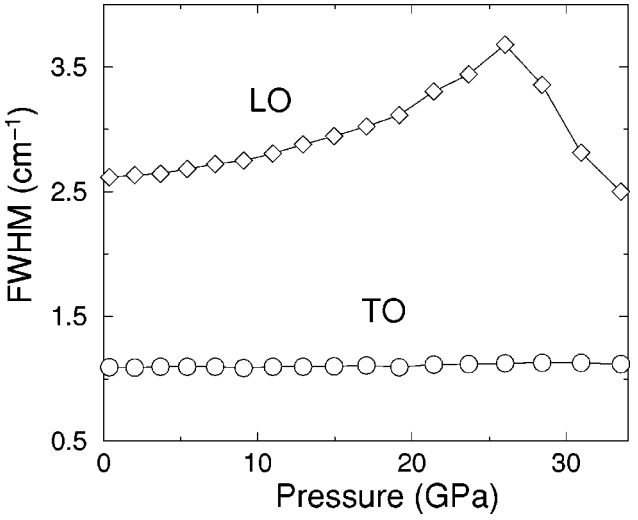

FIG. 6. Theoretical linewidths of the TO and LO zone-center optical modes of 3*C*-SiC for pressures up to 33 GPa.

up to 20 GPa at room temperature yield a rather weak pressure dependence of the TO and LO Raman linewidths.

The results of our calculations for the linewidths of TO and LO optical phonons vs pressure are shown in Fig. 6. At ambient pressure we obtained $2\Gamma_{TO}=1.09$ cm^{-1} for the FWHM of TO phonon and $2\Gamma_{LO}=2.62$ cm^{-1} for the LO mode. The agreement with zero-pressure experimental data is satisfactory, especially for the linewidth of the LO phonon (in spite of having neglected the anharmonicity related to the polarization which accompanies the LO phonon).

In the pressure range in which the linewidths were measured (see Fig. 5) theoretical and experimental data agree for the FWHM of the LO phonon. For $2\Gamma_{TO}$, the difference between experimental and theoretical values increases slightly with increasing pressure. One possible explanation is that above about 12 GPa we are at the limit of uniform and/or isotropic pressure conditions even when using He as a pressure transmitting medium. Therefore, for higher pressures small nonuniform or nonisotropic strain components produced during pressure changes at 300 K can lead to an increase in the measured linewidths arising from a small splitting of the twofold degenerate TO mode. On the other hand, it has been demonstrated recently[41] that even small deviations of calculated phonon frequencies from experimental values can cause considerable discrepancies in the absolute values and the pressure dependences of phonon linewidths.

B. Decay channels at ambient pressure

The theoretical calculations provide us with detailed information on the optical-phonon decay channels. We first consider the situation at ambient pressure.

The frequency difference between TO and LO phonons implies that the allowed decay processes should show substantial differences because of the differences in the density of final (two-phonon) states. To identify the dominant two-phonon processes involved we have computed the relative weight of the different decay channels, restricting the sum over j's in Eq. (1) to the individual final-state bands labeled ''TA'' ($j=1,2$), ''LA'' ($j=3$), and ''TO'' ($j=4,5$). The

TABLE IV. Calculated FWHM (2Γ) of the zone-center transverse and longitudinal optical phonons in $3C$-SiC for different pressures ($T=0$ K). The relative contribution of the various decay channels to the linewidths (in %) is also given.

Mode	P (GPa)	2Γ (cm^{-1})	LA+LA (%)	TA+TA (%)	LA+TA (%)
TO	0.0	1.09	8.6	24.8[a]+29.2	37.4
TO	33.5	1.12	6.5	21.9[a]+8.9	62.7
LO	0.0	2.62	11.4	74.6	14.0
LO	26.0	3.68	6.6	84.2	9.2
LO	33.5	2.50	9.4	76.9	13.7

[a]Klemens channel, see text.

results are reported in Table IV. The channels which give the largest contribution to the TO linewidth (54%) correspond to decay into TA branches only. This contribution consists of a decay into two phonons of the same branch (24%), called the *Klemens channel*,[49] and of decay into different TA branches (29%). The anharmonic decay of the LO phonon involves different channels: while the decay LO$\rightarrow$ TA + TA is kinematically forbidden by energy conservation, the decay into one transverse optical and one acoustic branch, longitudinal or transverse (LTA), is allowed.

In order to sharpen up our analysis we introduce the *frequency-resolved final-state spectral function*, $\gamma(\omega)$,[23] representing the probability per unit time that a TO (or LO) phonon decays into two modes of frequency ω and $\omega_{TO}-\omega$ ($\omega_{LO}-\omega$), respectively. Computationally, we obtain $\gamma(\omega)$ by inserting $\delta(\omega-\omega_{j_1}(\mathbf{q}))$ in Eq. (1) behind the summation sign.[50] The spectral function, $\gamma(\omega)$ of a TO (LO) phonon is symmetrical around the frequency $\omega_{TO}/2$ ($\omega_{LO}/2$). Integration over the whole phonon frequency range gives the value of the FWHM. We display the results obtained for TO and LO phonons in Fig. 7 together with the one-phonon density of states (dashed line). The central peak in the TO-$\gamma(\omega)$, at the frequency $\omega_{TO}/2$, corresponds to the Klemens channel and gives approximately one-third of the total contribution to the linewidth, the remaining contribution corresponding to decay into two phonon of different branches (the two small peaks close to the principal one).

The decay of an LO phonon shows a completely different picture, the dominant mechanism being the decay into different acoustic branches (the highest peaks in Fig. 7), while the Klemens channel gives only one-tenth of the total width. The additional side peaks correspond to decay processes which involve a transverse optical branch.

C. Decay channels under pressure

We now examine the behavior of the FWHM predicted by the theory at higher pressure. While the calculated transverse phonon linewidth of Fig. 6 remains practically unchanged, that of the LO phonon shows a monotonic increase up to 26 GPa, followed by a rapid decrease beyond this pressure. To understand this anomalous behavior we have considered the expression appearing in the right-hand side (rhs) of Eq. (1) after the summation sign, and performed the sum over branch indices, the resulting quantity depends on $\mathbf{q}$ and is thus called *wave vector resolved spectral function*.[23] Because of the energy conservation expressed by the Dirac delta function, the only region of the BZ which contributes to the FWHM is a 3D surface; we display the intersection of this surface with several high symmetry planes of the BZ in Fig. 8 for three different pressures. The magnitude of the anharmonic term at the 3D energy conservation surface is represented by a rainbow color scale that ranges from red to violet in order of increasing magnitude.

The rather large slope of the acoustic branches near the Brillouin-zone center results in a multiplicity of decay channels, as one can easily realize by looking at Fig. 8: all combinations of acoustic branches are allowed by conservation of energy as decay channels; they result in shapes of the LO and TO phonons different from those found in the other compound semiconductors investigated in Ref. 26. Moreover, the FWHM of the TO and LO modes show rather dif-

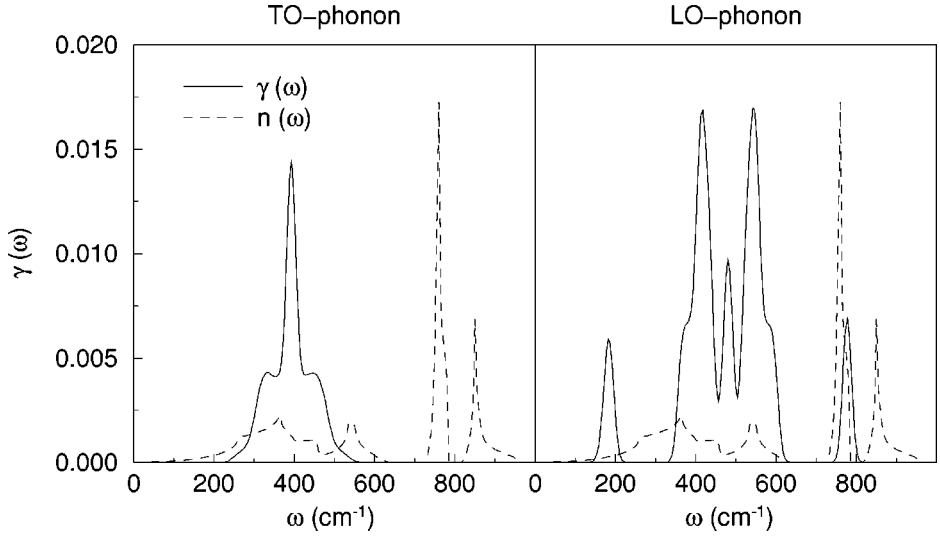

FIG. 7. Theoretical frequency-resolved spectral function $\gamma(\omega)$ (solid line) for TO and LO phonons of $3C$-SiC at zero temperature and pressure. For comparison, the corresponding one-phonon density of states $n(\omega)$ (dashed line, in arbitrary units) is also shown.

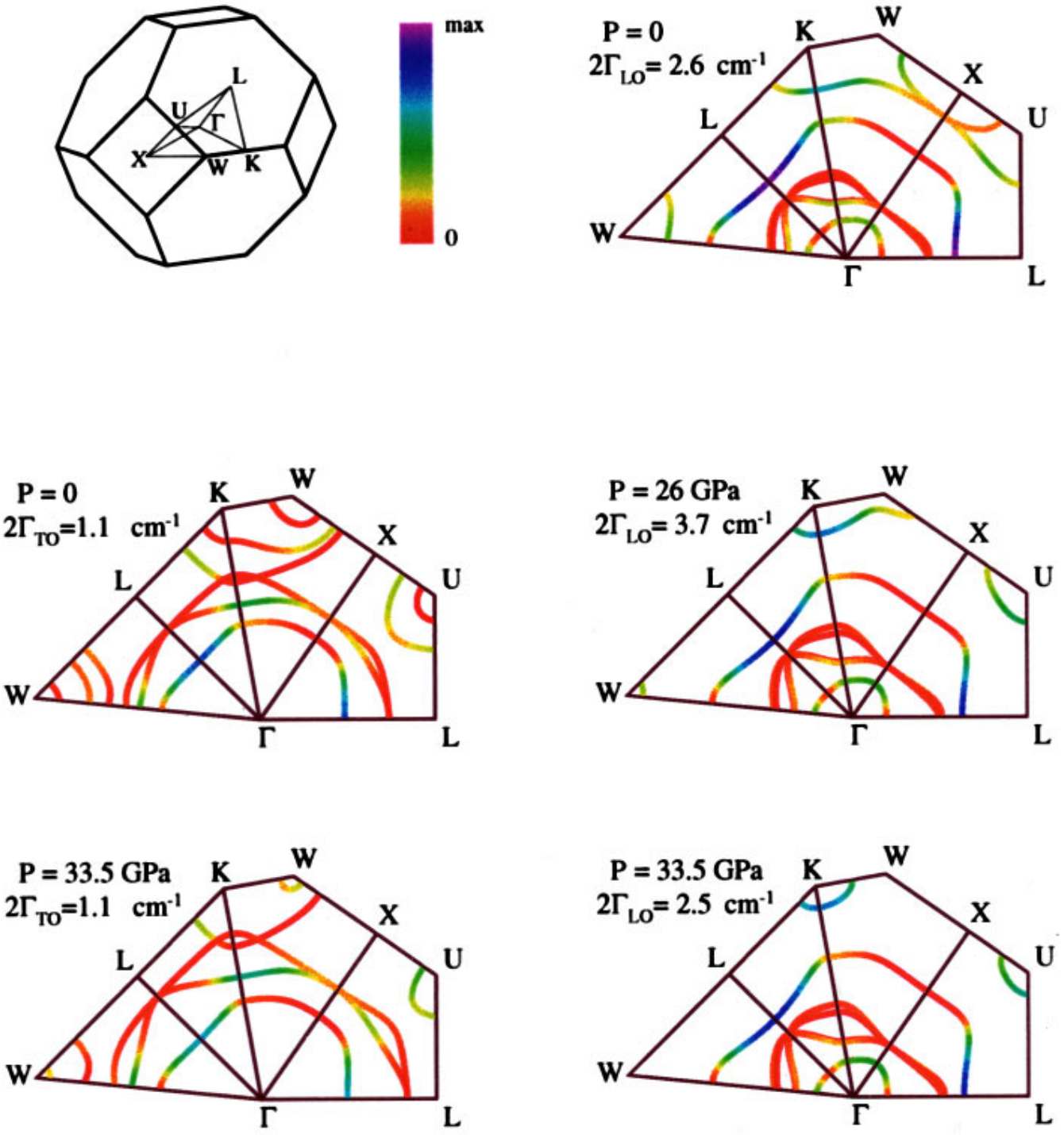

FIG. 8. (Color) Wave-vector-resolved final states for the decay of zone-center longitudinal and transverse optical modes at different pressures. On top: sketch of the Brillouin zone and color scale. Left column: color maps at $P=0$ and at 33.5 GPa for the linewidths of the TO phonon. Right column: color maps corresponding to the pressure $P=0$, 26, and 33.5 GPa for the linewidths of the LO phonon. The color scale goes from red to violet in order of increasing magnitude.

ferent behaviors. Since the frequencies are different, conservation of energy requires different decay channels.

At ambient pressure we can identify, among others, three decay channels close to the BZ center (the Γ point) corresponding to the decay of the LO phonon into TA and TO phonons. These channels contribute only a few percent to the linewidth. The smallness of this contribution is a consequence of translational invariance[26] which forces the coupling coefficients to vanish for $\omega \rightarrow 0$ for decay into acoustic phonons. The closed contour lying approximately halfway between the BZ center and its edge corresponds to decay processes involving the same acoustic branch, while the remaining channels, close to the BZ border, are due to LO $\rightarrow$ LA + TA processes. The latter are responsible for the main contribution to the LO phonon width. The relative weights calculated for the individual decay channels at dif-

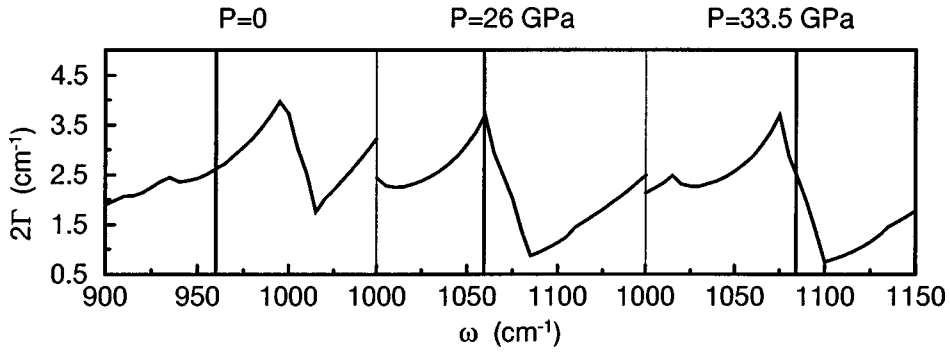

FIG. 9. Frequency-resolved FWHM at different pressures. The vertical lines indicate the corresponding LO frequencies.

ferent pressures are reported in Table IV. The evolution of the allowed decay channels under pressure can be followed by looking at the plots on Fig. 8 for $P=26$ GPa and $P=33$ GPa. The sharp decrease in slope of the FWHM above 26 GPa, displayed in Fig. 6, corresponds to *deactivating* the decay channel around the W point (see Fig. 8), i.e., the decay into phonons around the W point of the BZ, which becomes forbidden by energy conservation for pressures higher than 26 GPa.

For confirmation we can look at the frequency-resolved width, $\Gamma(\omega)$, which is obtained by substituting in the rhs of Eq. (1) the LO frequency ω_{LO} with variable ω ranging over the entire spectrum of frequencies. $\Gamma(\omega)$ is plotted in Fig. 9 for the three pressures under consideration, in the range of frequencies around ω_{LO}. When the frequency in the argument $\Gamma(\omega)$ corresponds to ω_{LO} we obtain the FWHM of the longitudinal mode. This FWHM can be found graphically from Fig. 9, by looking at the intersection of $\Gamma(\omega)$ with the vertical lines corresponding to the value of ω_{LO} at the given pressure. The shapes of $\Gamma(\omega)$ at the three different pressures are quite similar, the peaks, present in all the three plots of $\Gamma(\omega)$, correspond to the sum of the TA + LA frequencies at the W point of the BZ.

The peak in $\Gamma(\omega)$ shown in Fig. 9 arises from the van Hove singularity in the two-phonon density of states which corresponds to the LA+TA sum frequency at W. In fact, if in Eq. (1) we assume that the anharmonic potential V_3 is constant, the resulting expression becomes proportional to the two-phonon density of state. This confirms our previous assertion that the general behavior of Γ vs pressure is mainly driven by energy conservation, and supports the validity of the ZFAA made to compute the LO linewidth. Since we are not close to a phase transition [which occurs at about 100 GPa (Ref. 51)] the error with which the frequencies are computed (a few percent) can only shift the kink in the slope of the FWHM vs pressure to higher or lower pressures. Unfortunately, to the best of our knowledge, no experimental data have been reported in the literature concerning the frequencies of acoustic modes at W. Therefore, it is not possible to perform an analysis similar to that performed in Ref. 41 to predict the exact pressure at which the change of slope should be found experimentally.

Finally, we examine the decay channels corresponding to the FWHM of the TO phonon. The different channels can be easily identified in Fig. 8. At ambient pressure, going from the BZ center to the border we encounter the LA+LA channel plus two channels on LA+TA, while the TA+TA channels (the remaining lines) are allowed only around a few high symmetry points at the BZ border. The LA+LA channel displays a large anharmonic matrix element V_3 (the blue line that intersects the $\Gamma-L$ direction) but the constant energy surface is rather small and contributes less than 10% to the FWHM. By analyzing Fig. 8 we can understand the flat behavior of our computed FWHM vs pressure: according to our calculation it results from two competing mechanisms: with increasing pressure the channel TA+TA becomes forbidden by conservation of energy, having disappeared at 33.5 GPa. The channel LA+TA becomes more important because the corresponding constant energy surface increases (it moves closer to the BZ border).

V. CONCLUDING REMARKS

The two main conclusions from the combined experimental and first-principles theoretical study of phonon lifetimes in cubic SiC are: (1) The present experiments do not confirm the sharp increase in Raman linewidths near 10.6 GPa reported in an earlier high-pressure study.[3] Instead, the TO and LO linewidths behave rather smoothly in our experiments up to 15 GPa, increasing by less than 20% in this pressure range. A key feature in the present experiments is that helium was used as a pressure medium in order to ensure the smallest deviation from truly hydrostatic conditions at low temperatures. (2) The theoretical calculations of anharmonic effects presented here are found to be in good agreement with experiment, not only at zero pressure but also with respect to pressure-induced changes. This applies to the pressure dependence of optical phonon frequencies and, more important in the present context, to the phonon lifetimes as a function of pressure. Furthermore, the first-principles calculations enabled us to analyze in detail the different anharmonic decay channels limiting the intrinsic phonon lifetimes and to give reliable predictions on the pressure range where the experimental data are lacking.

ACKNOWLEDGMENTS

Thanks are due to W. J. Choyke for providing the cubic SiC crystals and W. Kress for a critical reading of the manuscript.

[1] P. T. B. Shaffer, Acta Crystallogr., Sect. B: Struct. Crystallogr. Cryst. Chem. **25**, 477 (1969).
[2] R. F. Davis, Z. Sitar, B. E. Williams, H. S. Kong, H. J. Kim, J. W. Palmour, J. A. Edmond, J. Ryu, J. T. Glass, and C. H. Carter, Jr., Mater. Sci. Eng., B **1**, 77 (1988).
[3] D. Olego and M. Cardona, Phys. Rev. B **25**, 1151 (1982).
[4] D. Olego, M. Cardona, and P. Vogl, Phys. Rev. B **25**, 3878 (1982).
[5] D. Olego and M. Cardona, Phys. Rev. B **25**, 3889 (1982).
[6] S. S. Mitra, O. Brafman, W. B. Daniels, and R. K. Crawford, Phys. Rev. **186**, 942 (1969).
[7] I. V. Aleksandrov, A. F. Goncharov, S. M. Stishov, and E. V. Yakovenko, Pis'ma Zh. Éksp. Teor. Fiz. **50**, 116 (1989) [JETP Lett. **50**, 127 (1989)].
[8] A. F. Goncharov, E. V. Yakovenko, and S. M. Stishov, Pis'ma Zh. Éksp. Teor. Fiz. **52**, 1092 (1990) [JETP Lett. **52**, 491 (1990)].
[9] G. Salvador and W. F. Sherman, J. Mol. Struct. **247**, 373 (1991).
[10] M. Kobayashi, R. Akimoto, S. Endo, M. Yamanaka, M. Shinohara, and K. Ikoma, in *Amorphous and Crystalline Silicon Carbide III and Other Group IV-IV Materials*, edited by G. L. Harris, Michael Spencer, and C. Y. Yang, Springer Proceeding in Physics Vol. 56 (Springer-Verlag, Berlin, 1991), p. 263.
[11] J. Liu and Y. K. Vohra, Phys. Rev. Lett. **72**, 4105 (1994).
[12] K. J. Chang and M. L. Cohen, Phys. Rev. B **35**, 8196 (1987).
[13] K. Karch, P. Pavone, W. Windl, O. Schütt, and D. Strauch, Phys. Rev. B **50**, 17 054 (1994).
[14] T. Sengstag, N. Binggeli, and A. Baldereschi, Phys. Rev. B **52**, R8613 (1995).
[15] K. Karch, F. Bechstedt, P. Pavone, and D. Strauch, Phys. Rev. B **53**, 13 400 (1996); J. Phys.: Condens. Matter **8**, 2945 (1996); K. Karch and F. Bechstedt, Europhys. Lett. **35**, 195 (1996).
[16] C.-Z. Wang, R. Yu, and H. Krakauer, Phys. Rev. B **53**, 5430 (1996).
[17] G. Wellenhofer, K. Karch, P. Pavone, U. Rössler, and D. Strauch, Phys. Rev. B **53**, 6071 (1996).
[18] See, for example, J. A. Kash and J. C. Tsang, in *Light Scattering in Solids VI*, edited by M. Cardona and G. Güntherodt (Springer-Verlag, Berlin, 1991), p. 423.
[19] A. Debernardi and M. Cardona, Nuovo Cimento D **20**, 923 (1998). Note that Fig. 4 in this reference indicates the absence of inhomogeneous broadening since the experimental points can be fitted to a standard Bose-Einstein-type temperature dependence without need of an inhomogeneous effect.
[20] For a complete expression see, e.g., J. Menéndez and M. Cardona, Phys. Rev. B **29**, 2051 (1984), and references therein.
[21] X. Gonze and J. P. Vigneron, Phys. Rev. B **39**, 13 120 (1989).
[22] A. Debernardi and S. Baroni, Solid State Commun. **91**, 813 (1994).
[23] A. Debernardi, S. Baroni, and E. Molinari, Phys. Rev. Lett. **75**, 1819 (1995).
[24] R. Resta, Phys. Rev. B **27**, 3620 (1983).
[25] R. M. Pick, M. H. Cohen, and R. M. Martin, Phys. Rev. B **1**, 910 (1970).
[26] A. Debernardi, Phys. Rev. B **57**, 12 847 (1998).
[27] See, e.g., *Theory of the Inhomogeneous Electron Gas*, edited by S. Lunquist and N. H. March (Plenum, New York, 1983), and references therein.
[28] D. R. Hamann, M. Schlüter, and C. Chiang, Phys. Rev. Lett. **43**, 1494 (1979); G. B. Bachelet, D. R. Hamann, and M. Schlüter, Phys. Rev. B **26**, 4199 (1982).
[29] P. Giannozzi, S. de Gironcoli, P. Pavone, and S. Baroni, Phys. Rev. B **43**, 7231 (1991).
[30] D. M. Ceperley and B. J. Alder, Phys. Rev. Lett. **45**, 566 (1980).
[31] J. P. Perdew and A. Zunger, Phys. Rev. B **23**, 5048 (1981).
[32] A. Baldereschi, Phys. Rev. B **7**, 5212 (1973); D. J. Chadi and M. L. Cohen, *ibid.* **8**, 5747 (1973); D. J. Chadi, *ibid.* **16**, 1746 (1977).
[33] H. J. Monkhorst and J. D. Pack, Phys. Rev. B **13**, 5188 (1976).
[34] G. Lehmann and M. Taut, Phys. Status Solidi B **54**, 469 (1972).
[35] O. Jepsen and O. K. Andersen, Solid State Commun. **9**, 1763 (1971).
[36] F. D. Murnaghan, Proc. Natl. Acad. Sci. USA **30**, 244 (1944).
[37] *Numerical Data and Functional Relationships in Science and Technology*, Landolt-Börnstein New Series, 17a, edited by O. Madelung (Springer-Verlag, Berlin, 1982), p. 136.
[38] P. Loubeyre, J. M. Besson, J. P. Pinceaux, and J. P. Hansen, Phys. Rev. Lett. **49**, 1172 (1982).
[39] G. J. Piermarini, S. Block, J. P. Barnett, and R. A. Forman, J. Appl. Phys. **46**, 2774 (1975); H. K. Mao, J. Xu, and P. M. Bell, J. Geophys. Res. **91**, 4673 (1986).
[40] S. Buchsbaum, R. L. Mills, and D. Schiferl, J. Phys. Chem. **88**, 2522 (1984).
[41] C. Ulrich, E. Anastassakis, K. Syassen, A. Debernardi, and M. Cardona, Phys. Rev. Lett. **78**, 1283 (1997).
[42] F. Engelbrecht, J. Zeman, G. Wellenhofer, C. Peppermüller, R. Helbig, G. Martinez, and U. Rössler, Phys. Rev. B **56**, 7348 (1997).
[43] D. W. Posener, Aust. J. Phys. **12**, 184 (1959).
[44] If one assumes that the force constants are analytic functions of the lattice parameter, one can make a Taylor expansion with respect to the lattice parameter of the frequencies and related quantities. The lattice parameter is then related to the pressure through Murnaghan's equation.
[45] M. Hanfland, K. Syassen, S. Fahy, S. G. Louie, and M. L. Cohen, Physica B & C **139&140**, 516 (1986).
[46] Diamond: M. H. Grimsditch and A. K. Ramdas, Phys. Rev. B **11**, 3139 (1975); Si: J. J. Hall, Phys. Rev. **161**, 756 (1967); Ge: L. J. Bruner and R. W. Keyes, Phys. Rev. Lett. **7**, 55 (1961).
[47] See, for example, B. A. Weinstein and R. Zallen, in *Light Scattering in Solids IV*, edited by M. Cardona and G. Güntherodt (Springer-Verlag, Berlin, 1984), p. 463.
[48] M. Cardona, J. Phys. (Paris), Colloq. **45**, C8-29 (1984).
[49] P. G. Klemens, Phys. Rev. **148**, 845 (1966).
[50] The present calculation of $\gamma(\omega)$ has been performed by broadening $\delta(\omega-\omega_j)$ with a Gaussian whose width is 10 cm^{-1}.
[51] M. Yoshida, A. Onodera, M. Ueno, K. Takemura, and O. Shimomura, Phys. Rev. B **48**, 10 587 (1993).